FULL PAPER

Dalton
www.rsc.org/dalton

Evaluation of the influence of a thioether substituent on the solid state and solution properties of N_3S-ligated copper(II) complexes †

Kyle J. Tubbs,‡[a] Amy L. Fuller,‡[a] Brian Bennett,[b] Atta M. Arif,[c] Magdalena M. Makowska-Grzyska[a] and Lisa M. Berreau*‡[a]

[a] *Department of Chemistry and Biochemistry, Utah State University, Logan, UT, USA. E-mail: berreau@cc.usu.edu*

[b] *Department of Biophysics, Medical College of Wisconsin, 8701 Watertown Plank Road, Milwaukee, WI, USA. E-mail: bbennett@mcw.edu*

[c] *Department of Chemistry, University of Utah, Salt Lake City, UT, USA. E-mail: arif@chemistry.utah.edu*

Received 30th April 2003, Accepted 13th June 2003
First published as an Advance Article on the web 30th June 2003

Admixture of a N_3S(thioether) ligand having two internal hydrogen bond donors (pbnpa: *N*-2-(phenylthio)ethyl-*N*,*N*-bis-((6-neopentylamino-2-pyridyl)methyl)amine; ebnpa: *N*-2-(ethylthio)ethyl-*N*,*N*-bis-((6-neopentylamino-2-pyridyl)methyl)amine) with equimolar amounts of $Cu(ClO_4)_2 \cdot 6H_2O$ and NaX (X = Cl^-, NCO^-, or N_3^-) in CH_3OH/H_2O yielded the mononuclear Cu(II) derivatives [(pbnpa)Cu–Cl]ClO_4 (**1**), [(ebnpa)Cu–Cl]ClO_4 (**2**), [(pbnpa)Cu–NCO]ClO_4 (**3**), [(ebnpa)Cu–NCO]ClO_4 (**4**), [(pbnpa)Cu–N_3]ClO_4 (**5**), and [(ebnpa)Cu–N_3]ClO_4 (**6**). Each complex was characterized by FTIR, UV-VIS, EPR, and elemental analysis. Complexes **1**, **2**, **3** and **6** were characterized by X-ray crystallography. The structural studies revealed that [(pbnpa)Cu–X]ClO_4 derivatives (**1**, **3**) exhibit a distorted square pyramidal type geometry, whereas [(ebnpa)Cu–X]ClO_4 complexes (**2**, **6**) may be classified as distorted trigonal bipyramidal. EPR studies in CH_3OH/CH_3CN solution revealed that **1**–**6** exhibit an axial type spectrum with $g_{\|} > g_{\perp} > 2.0$ and $A_{\|} = 15$–17 mT, consistent with a square pyramidal based geometry for the Cu(II) center in each complex. A second species detected in the EPR spectra of **2** and **6** has a smaller $A_{\|}$ value, consistent with greater spin delocalization on to sulfur, and likely results from geometric distortion of the [(ebnpa)Cu(II)–X]$^+$ ions present in **2** and **6**.

Introduction

Within the active sites of the copper-containing enzymes dopamine β-monooxygenase (DβM) and peptidylglycine α-amidating enzyme (PAM), substrate oxidation is proposed to occur at a mononuclear nitrogen/sulfur(thioether)-ligated copper center.[1] The coordination environment of this copper ion is similar for both enzymes and appears to vary with the oxidation level of the metal center.[2,3] For oxidized DβM, the Cu_B coordination environment has been identified by copper K-edge EXAFS studies as being comprised of two/three histidine ligands and one/two water molecules.[2a] In the oxidized copper(II) form of PAM, the primary coordination sphere of Cu_M consists of two histidine nitrogens, a water molecule, and a weakly-coordinated methionine sulfur (Cu–S_{Met} ~2.7 Å).[3] It is generally believed that a similar long Cu–S_{Met} interaction is present in DβM, but is undetectable by EXAFS. Reduction of the copper ions in DβM and PAM yields Cu_B and Cu_M centers that both exhibit strong coordination to a methionine sulfur (Cu_B Cu–S_{Met}: 2.25 Å (EXAFS);[2a] Cu_M: Cu–S_{Met}: 2.24 Å (EXAFS)[2b,4]) as well as two histidine nitrogens.[5] These changes in Cu–S_{Met} interactions in DβM and PAM, as a function of the oxidation state of the metal, have been suggested to be important toward tuning the redox potential of the copper center.[2b]

A recent model study suggests that the influence of thioether ligation on the chemistry of divalent copper centers remains to be fully elucidated.[6,7] Specifically, an investigation by Kodera and coworkers suggests that the nature of the thioether substituent in supporting N_3S chelate ligands is important toward influencing the chemistry of copper(II) species.[6e] Using a series of *S*-substituted N_3S ligands (2-bis-(6-methyl-2-pyridylmethyl)-amino-1-(R-)ethane, R = $–SC_6H_5$, $–SCH_3$, $–S(i\text{-}C_3H_7)$), Kodera *et al.* found that their ability to spectroscopically observe a novel Cu–OOH intermediate was related to the nature of the thioether substituent present, with a phenyl thioether ligand providing a spectroscopically observable CuO_2H derivative. Notably, ligands having $–SCH_3$ and $–S(i\text{-}C_3H_7)$ substitutents were not effective in producing a spectroscopically observable CuO_2H intermediate. A copper(II) chloride complex of the 2-bis-(6-methyl-2-pyridylmethyl)amino-1-(phenylthio)ethane ligand was shown to exhibit a distorted square pyramidal geometry (τ = 0.39)[8] with a long axial Cu–S(thioether) interaction (Cu–S 2.6035(3) Å). This distance is slightly shorter than that observed for the Cu_M–S_{Met} interaction (~2.7 Å) in the oxidized form of PAM.[3] The structures of mononuclear divalent copper complexes of other N_3S ligands involved in the study by Kodera *et al.* (*e.g.* $–SCH_3$, $S(i\text{-}C_3H_7)$ derivatives) were not reported. Thus, it is unclear whether the phenylthio substituent was the only supporting chelate ligand in the above outlined series of ligands to yield a weak Cu–S(thioether) interaction in copper(II) derivatives. Another observation regarding the 2-bis-(6-methyl-2-pyridylmethyl)amino-1-(phenylthio)ethane-ligated copper system of Kodera *et al.* is that the phenyl thioether substituent does not undergo sulfur oxidation in the presence of H_2O_2. Copper complexes having a $–SCH_3$ and $–S(i\text{-}C_3H_7)$ substituent in the supporting chelate ligand were instead observed to readily undergo sulfur oxidation to yield sulfoxides and sulfones under identical conditions.[6e]

In the work described herein, we have examined the fundamental copper(II) coordination chemistry of two N_3S ligands having two internal hydrogen bond donors. In the context of this study, we have addressed an issue that is of relevance to the previously reported study by Kodera and coworkers.[6e] Specifically, we have directed our studies toward evaluating how different thioether substituents influence the solid state and solution properties of mononuclear divalent copper complexes relevant to the Cu_B and Cu_M sites in DβM and PAM, respectively.

† Electronic supplementary information (ESI) available: plot of $A_{\|}$ *vs.* $g_{\|}$. See http://www.rsc.org/suppdata/dt/b3/b304846b/
‡ These authors contributed equally to this work.

DOI: 10.1039/b304846b

Table 1 Crystal data, data collection, and refinement parameters for **1**, **2**, **3**, and **6**[a]

	1	**2**	**3**	**6**
Formula	$C_{30}H_{43}Cl_2CuN_5O_4S$	$C_{26}H_{43}Cl_2CuN_5O_4S$	$C_{31}H_{43}ClCuN_6O_5S$	$C_{26}H_{43}ClCuN_8O_4S$
M	704.19	656.15	710.76	662.73
Crystal system	Monoclinic	Triclinic	Monoclinic	Triclinic
Space group	$P2(1)/c$	$P\bar{1}$	$P2(1)/c$	$P\bar{1}$
a/Å	11.0077(2)	8.4860(1)	7.2979(2)	8.5866(2)
b/Å	14.5441(2)	13.8394(2)	34.5443(14)	13.7903(3)
c/Å	20.7276(5)	14.3749(3)	13.0965(5)	14.6773(4)
α/°		101.7717(6)		78.9526(9)
β/°	97.4909(7)	91.7414(6)	91.517(3)	89.4294(9)
γ/°		106.5561(11)		73.8704(16)
V/Å^3	3290.11(11)	1577.11(4)	3300.5(2)	1636.89(7)
Z	4	2	4	2
μ/mm^{-1}	0.932	0.967	0.855	0.856
T/K	200(1)	150(1)	150(1)	150(1)
Reflns measured	13782	11542	10159	11484
Unique reflns obs.	7509	7142	6643	7415
R_1	0.0462	0.0321	0.0499	0.0405
wR_2	0.1027	0.0723	0.0911	0.0969

[a] All structures determined using Mo Kα radiation, refinements based on F^2. For $I > 2\sigma(I)$, $R_1 = \Sigma||F_o| - |F_c||/\Sigma|F_o|$, and $wR_2 = [\Sigma[w(F_o^2 - F_c^2)^2/\Sigma[(F_o^2)^2]]^{1/2}$, where $w = 1/[\sigma^2(F_o^2) + (aP)^2 + bP]$.

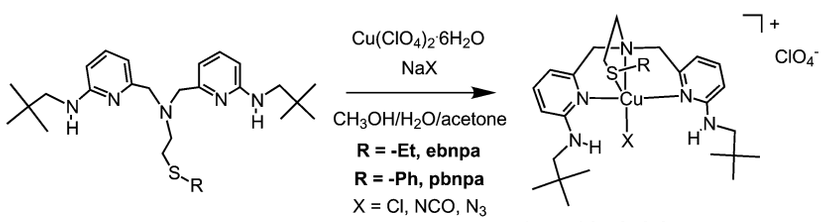

[(pbnpa)Cu-Cl]ClO_4 (**1**, 71%)
[(ebnpa)Cu-Cl]ClO_4 (**2**, 90%)
[(pbnpa)Cu-NCO]ClO_4 (**3**, 86%)
[(ebnpa)Cu-NCO]ClO_4 (**4**, 81%)
[(pbnpa)Cu-N_3]ClO_4 (**5**, 69%)
[(ebnpa)Cu-N_3]ClO_4 (**6**, 91%)

Scheme 1

Results and discussion

Syntheses and structures

Treatment of a N_3S ligand having two internal hydrogen bond donors (pbnpa or ebnpa[9]) with equimolar amounts of $Cu(ClO_4)_2 \cdot 6H_2O$ and NaX (X = Cl, NCO, N_3) in methanol, followed by crystallization from methanol/water/acetone, yielded a series of crystalline solids (**1**–**6**, Scheme 1) following partial evaporation of the solutions at ambient temperature. Each solid was carefully dried under vacuum and characterized by FTIR, UV-VIS, EPR, and elemental analysis.

Crystals suitable for single crystal X-ray crystallographic analysis were obtained for complexes **1**, **2**, **3**, and **6**. Details of the data collection and structure refinement are given in Table 1. Structural drawings of the complexes are shown in Fig. 1 and 2. Selected bond distances and angles are given in Table 2.

The structural features of [(pbnpa)Cu–Cl]ClO_4 (**1**) are generally similar to the chloride complex reported by Kodera and coworkers supported by the 2-bis-(6-methyl-2-pyridylmethyl)-amino-1-(phenylthio)ethane chelate ligand (L1).[6e] However, subtle differences are present, including a slightly longer Cu–SPh interaction (**1**: Cu(1)–S(1) 2.6605(8) Å; [(L1)CuCl]ClO_4: Cu–S 2.6035(3) Å) a more square pyramidal Cu(II) center (**1**: τ = 0.25; [(L1)CuCl]ClO_4: τ = 0.39),[8] and a slightly longer Cu–Cl bond (**1**: Cu(1)–Cl(1) 2.2548(8) Å; [(L1)CuCl]ClO_4: Cu–Cl(1) 2.2159(3) Å). Notably, the Cu–S(1) distance of **1** is ~0.1 Å shorter than that observed for a mononuclear N_3S-ligated copper(II) bromide complex of the methyl thioether ligand *N*-2-(methylthio)ethyl-*N*,*N*-bis-(2-pyridylmethyl)amine (L2, [(L2)Cu–Br]ClO_4: Cu–S(1) 2.762(3) Å, τ = 0.19).[8,10] Significant solid-state structural perturbation is found when the phenyl thioether moiety in **1** is replaced by an ethyl thioether substituent. In the X-ray crystal structure of [(ebnpa)Cu–Cl]ClO_4 (**2**), the geometry of the copper(II) ion is distorted trigonal bipyramidal (τ = 0.63),[8] with the Cu(1)–S(1) bond length (2.3681(5) Å) being ~0.29 Å shorter than that observed for **1**. This Cu(II)–S(thioether) distance is only slightly longer than that observed for a distorted square pyramidal (τ = 0.15)[8] copper(II) complex of the N_3S ligand *N*-2-(methylthio)ethyl-*N*,*N*-bis-(2-pyridylethyl)amine (2.335(2) Å), wherein a pyridyl nitrogen is found in the axial position (Cu–N 2.199(4) Å).[6c] The Cu–N_{py} distances in **2** are elongated by ~0.07–0.11 Å as compared to those found in **1**, with the longest being Cu(1)–N(1) (2.1744(14) Å).

On the basis of comparison of R and $U(B)$ values for structure solutions for **3** as [(pbnpa)Cu–NCO]ClO_4 or [(pbnpa)-Cu–OCN]ClO_4, we have concluded that the cyanate ligand exhibits *N*-coordination. Overall, as in **1**, the copper(II) center of **3** exhibits a slightly distorted square pyramidal geometry (τ = 0.08).[8] The Cu(1)–S(1) distance (2.7143(9) Å) is ~0.05 Å longer than for the chloride derivative. The Cu–N distances involving the chelate ligand for **1** and **3** are identical within experimental error. The Cu(1)–N(6) distance (1.943(3) Å) is at the long end of the range (~1.89–1.96 Å) of Cu–N(NCO) equatorial bond lengths reported in the literature.[11] The Cu(1)–N(6)–C(31) angle (140.1(3)°) is acute when compared to other complexes having terminal cyanate coordination to a copper(II) center. (~138–170°) and thus suggests a major contribution of resonance form **A** (below) in the cyanate bonding in **3**.[11] This notion is supported by the observation of identical N(6)–C(31)

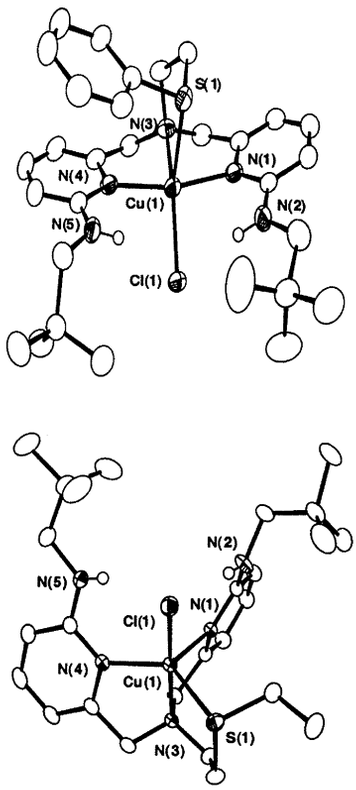

Fig. 1 Representations of the cationic portions of the X-ray crystal structures of **1** (top) and **2** (bottom). All ellipsoids are shown at the 50% probability level (all hydrogen atoms except secondary amine hydrogens not shown for clarity).

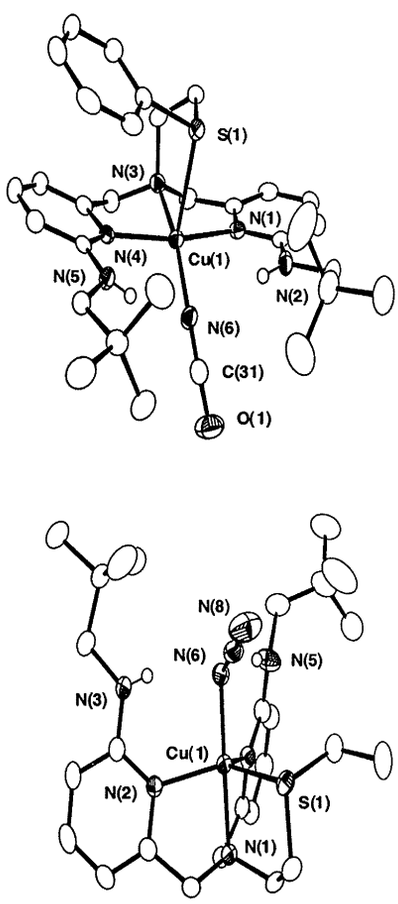

Fig. 2 Representations of the cationic portions of the X-ray crystal structures of **3** (top) and **6** (bottom). All ellipsoids are shown at the 50% probability level (all hydrogen atoms except secondary amine hydrogens not shown for clarity).

Table 2 Selected bond distances (Å) and angles (°) for the X-ray structures of **1**, **2**, **3**, and **6**[a]

1		**2**	
Cu(1)–N(1)	2.025(2)	Cu(1)–N(1)	2.1744(14)
Cu(1)–N(3)	2.043(2)	Cu(1)–N(3)	2.0374(15)
Cu(1)–N(4)	2.014(2)	Cu(1)–N(4)	2.0897(14)
Cu(1)–Cl(1)	2.2548(8)	Cu(1)–Cl(1)	2.2740(5)
Cu(1)–S(1)	2.6605(8)	Cu(1)–S(1)	2.3681(5)
Cl(1)–Cu(1)–N(1)	98.26(7)	Cl(1)–Cu(1)–N(1)	105.84(4)
Cl(1)–Cu(1)–N(3)	149.82(7)	Cl(1)–Cu(1)–N(3)	171.75(4)
Cl(1)–Cu(1)–N(4)	95.59(7)	Cl(1)–Cu(1)–N(4)	101.48(4)
Cl(1)–Cu(1)–S(1)	123.37(3)	Cl(1)–Cu(1)–S(1)	86.614(17)
N(1)–Cu(1)–N(4)	165.08(9)	N(1)–Cu(1)–N(4)	109.59(6)
N(1)–Cu(1)–S(1)	81.25(7)	N(1)–Cu(1)–S(1)	111.45(4)
N(4)–Cu(1)–S(1)	95.76(7)	N(4)–Cu(1)–S(1)	133.97(4)
N(3)–Cu(1)–N(1)	82.46(9)	N(3)–Cu(1)–N(1)	80.35(6)
N(3)–Cu(1)–N(4)	82.78(9)	N(3)–Cu(1)–N(4)	81.12(6)
N(3)–Cu(1)–S(1)	86.68(7)	N(3)–Cu(1)–S(1)	86.01(4)
3		**6**	
Cu(1)–N(1)	2.017(3)	Cu(1)–N(1)	2.0214(18)
Cu(1)–N(3)	2.040(3)	Cu(1)–N(2)	2.0950(17)
Cu(1)–N(4)	2.029(3)	Cu(1)–N(4)	2.1474(19)
Cu(1)–N(6)	1.943(3)	Cu(1)–N(6)	1.9652(19)
Cu(1)–S(1)	2.7143(9)	Cu(1)–S(1)	2.4015(6)
N(6)–Cu(1)–N(1)	97.34(11)	N(1)–Cu(1)–N(6)	178.33(7)
N(6)–Cu(1)–N(3)	160.69(12)	N(2)–Cu(1)–N(6)	99.60(7)
N(6)–Cu(1)–N(4)	96.16(10)	S(1)–Cu(1)–N(6)	91.85(5)
N(6)–Cu(1)–S(1)	113.76(9)	N(2)–Cu(1)–N(4)	112.24(7)
N(1)–Cu(1)–N(4)	165.70(10)	N(2)–Cu(1)–S(1)	128.59(5)
N(1)–Cu(1)–S(1)	86.37(7)	N(4)–Cu(1)–S(1)	115.04(5)
N(4)–Cu(1)–S(1)	92.48(7)	N(1)–Cu(1)–N(2)	81.66(7)
N(3)–Cu(1)–N(1)	82.61(10)	N(1)–Cu(1)–N(4)	81.31(7)
N(3)–Cu(1)–N(4)	83.09(10)	N(1)–Cu(1)–S(1)	86.50(5)
N(3)–Cu(1)–S(1)	85.54(7)	N(4)–Cu(1)–N(6)	99.18(8)

[a] Estimated standard deviations are indicated in parentheses.

and C(31)–O(1) bond lengths for **3** within experimental error (1.189(4) and 1.199(4) Å, respectively), and a N(6)–C(31)–O(1) bond angle of 176.5(4)°.

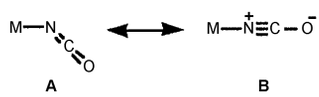

Azide anion is an inhibitor of DβM and has been used in kinetic, EPR, and paramagnetic NMR studies of the enzyme.[12] For this reason, we have comprehensively characterized copper(II) azide derivatives of the pbnpa and ebnpa ligands (**5** and **6**). Comparison of the X-ray crystallographically determined metrical parameters of **6** with those of $[Cu(Hbppa)(N_3)]ClO_4$, a mononuclear Cu(II) azide complex of a structurally related ligand (Hbppa = *N*-(2-pyridylmethyl)-*N*,*N*-bis(6-pivaloylamido-2-pyridylmethyl)amine)[13] that has previously been reported in the literature, reveals interesting perturbations due to substitution of a thioether for a pyridyl donor in the supporting chelate ligand. Specifically, the copper(II) ion in **6** exhibits a more trigonal bipyramidal geometry ($\tau = 0.83$; $[Cu(Hbppa)(N_3)]ClO_4$ $\tau = 0.65$),[8] a slightly elongated Cu–N(tertiary amine) distance (**6**: Cu(1)–N(1) 2.0214(18) Å; $[Cu(Hbppa)(N_3)]ClO_4$ 1.987(7) Å), and a significantly longer bonding interaction with the thioether sulfur (**6**: Cu(1)–S(1) 2.4015(6) Å) than is observed with the pyridyl nitrogen in $[Cu(Hbppa)(N_3)]ClO_4$ (2.056(7) Å). The Cu–N(azide) distances are similar for the two complexes (**6**: 1.9652 (19) Å; $[Cu(Hbppa)(N_3)]ClO_4$ 1.937(7) Å). Finally, the bond distances (N(6)–N(7) 1.212(3) Å, N(7)–N(8) 1.145(3) Å) and angles (Cu(1)–N(6)–N(7) 121.00(15)°, N(6)–N(7)–N(8) 178.1(2)°) involving the azide ligand in **6** are typical of transition metal azide ligation. Specifically, the longer N–N distance, due to contributions from the canonical form **A** (below), is found between the metal-bound nitrogen and the middle nitrogen, and the M–N_3 bond angle is ~117–132°.[14]

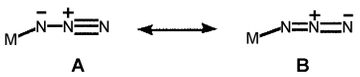

Evidence for hydrogen-bonding interactions between the neopentyl amine moieties of the pbnpa/ebnpa ligands and the bound anions (Cl^-, NCO^-, and N_3^-) may be derived from the solid state structures of **1**–**3** and **6**. For the chloride derivatives, the observed heteroatom distances (**1**: N(1) ··· Cl(1) 3.17 Å, N(5) ··· Cl(1) 3.17 Å; **2**: N(1) ··· Cl(1) 3.21 Å, N(5) ··· Cl(1) 3.20 Å) indicate that hydrogen-bonding interactions are likely present.[15] The same can be inferred for the cyanate and azide derivatives **3** (N(2) ··· N(6) 2.93 Å, N(5) ··· N(6) 2.89 Å) and **6** (N(2) ··· N(6) 2.91 Å, N(5) ··· N(6) 2.88 Å), albeit based on the bond distances/angles of these bound psuedohalides, only approximately one lone pair is available on the metal-bound nitrogen atom of either **3** or **6** to participate in secondary hydrogen bonding interactions.

FTIR, UV-VIS, and EPR spectroscopy

The ν_a(NCO) vibrations for **3** and **4** are found at 2191 and 2187 cm^{-1}, respectively. A ν_s vibration, which is typically found in the range of 1100–1400 cm^{-1}, is not readily identifiable in these systems due to overlap with ligand-based vibrations.

For the azide derivatives **5** and **6**, the $\nu_a(N_3)$ vibrations are found at 2051 and 2061 cm^{-1}, respectively. These values compare well with the same vibration observed for Cu(Et_4dien)-Br(N_3) (2053 cm^{-1}), a complex that possesses a terminal azide anion with symmetric N–N distances.[16] A $\nu_s(N_3)$ vibration was not identifiable (typically ~1300 cm^{-1}) upon comparison of the solid state FTIR spectra for chloride (**1** and **2**) and azide derivatives (**5** and **6**).

The region of 3400–3200 cm^{-1} in the solid state FTIR spectra for this family of complexes is complicated by the appearance of either two distinct bands, or one broad band that looks to be the overlap of two features. Small differences detected in the hydrogen-bonding interactions involving the bound halides/pseudohalides in **1**–**6** by X-ray crystallography may provide a rationale for the observation of two bands. However, as the heteroatom distances of these interactions differ by <0.05 Å, an alternative explanation could be that the band at lower frequency is an overtone of the N–H bending vibration (found in the region 1618–1624 cm^{-1} for **1**–**6**) which is intensified by Fermi resonance.[17]

In CH_3CN solution (~2–3 mM), the pbnpa-ligated complexes (**1**, **3**, and **5**) generally exhibit d–d transitions at higher energies, and with lower extinction coefficients, than the ebnpa-ligated analogs (**2**, **4**, and **6**; Fig. 3). LMCT features involving the

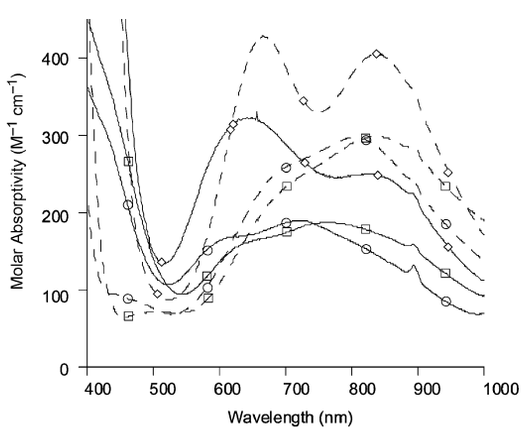

Fig. 3 UV-vis spectral features of **1**–**6** in d–d transition region. Complexes having pbnpa as the supporting chelate ligand are shown in solid lines (**1** (square), **3** (circle), **5** (diamond)); ebnpa-ligated systems are shown in dashed lines (**2** (square), **4** (circle), and **6** (diamond)).

Table 3 EPR parameters for **1**–**6**

Complex	$g_\parallel$	$g_\perp$	$A_\parallel$/mT	$A_\perp$/mT
1	2.245	2.049	15.4	[a]
2[b]	2.223	2.032	16.6	[a]
	2.192	2.054	12.0	[a]
3	2.250	2.047	15.9	1.1
4	2.248	2.052	16.8	1.3
5	2.248	2.050	15.7	1.2
6[b]	2.243	2.054	15.6	1.1
	2.167	–[c]	5.6	[a]

[a] None detected. [b] Two major species were identified by difference. [c] $g_\perp$ could not be determined.

bound anion were observed only for the azide derivatives (**5**: 388 nm (2200 M^{-1} cm^{-1}); **6**: 398 nm (2050 M^{-1} cm^{-1})).

EPR spectra collected on 0.4 mM solutions (9 : 1 CH_3OH : CH_3CN) of **1**–**6** yielded spectra as shown in Fig. 4. These spectra show species with clear $g(z) > g(x,y)$ and $A(z)$ coupling for all of the complexes, consistent with the presence of a $d_{x^2-y^2}$ ground state and a square pyramidal-based geometry in solution. Complexes **2** and **6** exhibit more complicated spectra, with two species present in each sample. Values for $g_\parallel$, $g_\perp$, $A_\parallel$, and $A_\perp$ for **1**–**6**, derived from spectral simulation,[18] are given in Table 3.

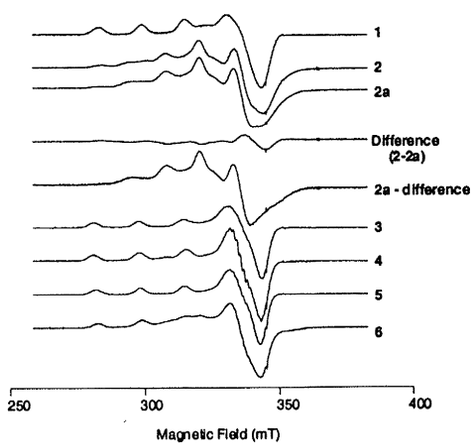

Fig. 4 Low temperature EPR spectra of complexes in frozen solution (0.4 mM in 9 : 1 CH_3OH : CH_3CN). Spectra are labelled according to compound number (**1**–**6**). Each trace (except **2a**) was recorded at 115 K, 2 mW microwave power, 9.32 GHz. Trace **2a** was recorded at 115 K, 159 mW microwave power. All traces are presented with principal *g*-values aligned to a magnetic field scale corresponding to a microwave frequency of 9.64 GHz.

Using an analysis of $g(z)$ and $A(z)$ values developed by Peisach and Blumberg,[19] we have determined that complexes **1** and **3**–**5** possess predominantly mixed nitrogen/oxygen ligation (Fig. S1, supplementary information †). Notably, this does not rule out the presence of a long Cu–S interaction in these systems, akin to that observed in the solid state structure of **1**. One component present in the EPR spectra of **2** and **6** may be classified in a similar manner. However, an additional species present in these samples has a smaller $A_\parallel$ value, consistent with greater spin delocalization on to sulfur.[19] These additional species likely result from geometric distortion of the Cu(II) cations present in **2** and **6**, and may be present only in the ebnpa-ligated systems (–SEt) due to an enhanced donor ability for the alkyl- *versus* an aryl-substituted thioether sulfur in the supporting chelate ligand.

Conclusions

In this study, we have examined the structural and solution properties of a new family of divalent copper complexes

supported by two N_3S(thioether) chelate ligands, each having two internal hydrogen bond donors. The N_3S ligands differ in the nature of the –SR substituent (R = Ph (pbnpa) or Et (ebnpa)). Single crystal X-ray crystallographic analysis of copper(II) chloride, cyanate, and azide derivatives revealed that –SPh ligated systems tend to produce copper(II) derivatives having a more square pyramidal structure and a long Cu–S interaction (~2.7 Å), whereas –SEt ligated systems exhibit a distorted trigonal bipyramidal geometry in the solid state. Solution EPR studies revealed that the species present for both –SPh and –SEt supported copper(II) complexes have a square pyramidal based geometry. Interestingly, only –SEt (ebnpa) derivatives have a second species present that exhibits an $A_{\|}$ value consistent with enhanced spin delocalization on sulfur. The subtle differences in solution behaviour between the –SPh and –SEt ligated systems may explain why the presence of a specific thioether substitutent has been observed to influence the chemistry of divalent copper complexes relevant to DβM and PAM.[6e]

Experimental

General

All reagents and solvents were obtained from commercial sources and were used as received unless otherwise noted. Solvent used in the preparation of the pbnpa ligand were dried according to literature procedures and were distilled under nitrogen prior to use.[20] The ligand ebnpa (*N*-2-(ethylthio)ethyl-*N*,*N*-bis-(6-neopentylamino-2-pyridymethyl)amine) and the ligand precursor 2-(phenylthio)ethylamine hydrochloride were prepared according to literature procedures.[9,21] FTIR and ^{1}H and ^{13}C{^{1}H} NMR spectra were collected under conditions identical to those previously reported.[22] EPR spectra were recorded using Bruker Elexsys E500 spectrometers equipped with either (1) a 9.64 GHz ER 4116DM cavity and an Oxford Instruments ESR-900 helium flow cryostat or, (2) a 9.32 GHz ER 4123SHQE cavity and an ER 4131VT nitrogen flow temperature control system. Magnetic fields and microwave frequencies were recorded and spectra are all presented on a field scale corresponding to 9.64 GHz. Spin Hamiltonian parameters were derived from data prior to field adjustment.[18] Elemental analyses were performed by Atlantic Microlabs of Norcross, GA.

Preparation of *N*-2-(phenylthio)ethyl-*N*,*N*-bis-((6-pivalolyl-amido-2-pyridyl)methyl)amine (pbppa)

Prepared in a similar manner to *N*-2-(ethylthio)ethyl-*N*,*N*-bis-((6-pivalolylamido-2-pyridyl)methyl)amine (ebppa), in this case using 2-(phenylthio)ethylamine hydrochloride.[9] Purified by column chromatography on 200–400 mesh silica gel (1 : 1 ethyl acetate: hexane; R_f = 0.40). Yield: 80%. Found: C, 67.61, H, 7.35, N, 13.04. $C_{30}H_{39}N_5SO_2$ requires C, 67.51, H, 7.37, N, 13.13%; ν_{max}/cm^{-1} 3436 (N–H), 1684 (C=O); ^{1}H NMR (CD_3CN, 270 MHz): δ 8.20 (br, 2H), 7.99 (d, J = 8.2 Hz, 4H), 7.67 (t, J = 7.6 Hz, 2H), 7.26 (m, 4H), 3.71 (s, 4H), 3.14–3.05 (m, 2H), 2.80–2.70 (m, 2H), 1.25 (s, 18H). ^{13}C{^{1}H} NMR (CD_3CN, 67.9 MHz) δ 178.0, 159.2, 152.2, 139.6, 137.5, 130.0, 129.0, 126.5, 119.6, 112.7, 61.0, 53.9, 40.5, 31.1, 27.6 (15 signals expected and observed); m/z 534 ([M + H]$^+$, 100%).

Preparation of *N*-2-(phenylthio)ethyl-*N*,*N*-bis-((6-neopentyl-amino-2-pyridyl)methyl)amine (pbnpa)

Prepared in a manner similar to *N*-2-(ethylthio)ethyl-*N*,*N*-bis-((6-neopenylamino-2-pyridyl)methyl)amine (ebnpa).[9] Purified by column chromatography on 200–400 mesh silica gel (R_f ~ 0.55 broad, trailing band). Yield: 55%. Found: C, 70.45, H, 8.67, N, 13.52. $C_{30}H_{43}N_5S$ requires C, 71.24, H, 8.58, N, 13.86%; ν_{max}/cm^{-1} (KBr) 3420 (N–H); ν_{max}/cm^{-1} (CH_2Cl_2, 100 mM) 3427; ^{1}H NMR (CD_3CN, 270 MHz): δ 7.32 (t, J = 7.2 Hz, 2H), 7.22–7.16 (m, 4H), 7.15–7.06 (m, 1H), 6.69 (d, J = 7.2 Hz, 2H), 6.32 (d, J = 8.2 Hz, 2H), 5.02 (br, 2H, N–*H*), 3.62 (s, 4H), 3.13 (d, J = 6.3 Hz, 4H), 3.14–3.06 (m, 2H), 2.82–2.72 (m, 2H), 0.92 (s, 18H). ^{13}C{^{1}H} NMR (CD_3CN, 67.9 MHz) δ 160.2, 158.6, 138.2, 137.9, 130.0, 128.9, 126.3, 111.8, 106.4, 61.0, 52.9, 53.5, 32.9, 31.3, 27.9 (15 signals expected and observed); m/z 506 ([M + H]$^+$, 100%).

Caution! Perchlorate salts of metal complexes with organic ligands are potentially explosive. Only small amounts of material should be prepared and these should be handled with great care.[23]

General procedure for preparation of copper(II) complexes

A methanol solution (~1 mL) of the chelate ligand (pbnpa or ebnpa, ~40–60 mg) was treated with an equimolar amount of $Cu(ClO_4)_2{\cdot}6H_2O$ dissolved in methanol (~1 mL). After stirring the resulting solution for ~10 min, a methanol slurry of NaX (X = Cl, NCO, N_3) was added. To this heterogeneous mixture was added water (~6 mL) and acetone (~3 mL) until a homogeneous solution was obtained. This solution was then allowed to evaporate at ambient temperature, which led to the deposition of **1**–**6** as crystalline solids.

[(pbnpa)Cu–Cl]ClO_4 (1)

Yield: 71%. Found: C, 51.04; H, 6.13; N, 9.88. $C_{30}H_{43}N_5O_4SCl_2Cu$ requires C, 51.27; H, 6.17; N, 9.97%; λ_{max}/nm (CH_3CN) 325 (ε/M^{-1} cm^{-1} 12 400), 670 (sh, 170), 765 (190); ν_{max}/cm^{-1} (KBr) 3321 (N–H), 1089 (ClO_4), 623 (ClO_4); m/z 603 ([M–ClO_4]$^+$, 100%).

[(ebnpa)Cu–Cl]ClO_4 (2)

Yield: 90%. Found: C, 47.51; H, 6.58; N, 10.51. $C_{26}H_{43}N_5O_4SCl_2Cu$ requires C, 47.69; H, 6.62; N, 10.70%; λ_{max}/nm (CH_3CN) 323 (ε/M^{-1} cm^{-1} 12 100), 740 (sh, 250), 837 (280); ν_{max}/cm^{-1} (KBr) 3298 (N–H), 1087 (ClO_4), 623 (ClO_4); m/z 555 ([M–ClO_4]$^+$, 100%).

[(pbnpa)Cu–NCO]ClO_4 (3)

Yield: 86%. Found: C, 51.60; H, 6.03; N, 11.55. $C_{31}H_{43}N_6O_5SClCu$ requires C, 52.45; H, 6.11; N, 11.85%; λ_{max}/nm (CH_3CN) 324 (ε/M^{-1} cm^{-1} 12 300), 628 (180), 719 (190); ν_{max}/cm^{-1} (KBr) 3352 (N–H), 2191 (NCO), 1088 (ClO_4), 622 (ν_{ClO_4}); m/z 610 ([M–ClO_4]$^+$, 55%).

[(ebnpa)Cu–NCO]ClO_4 (4)

Yield: 81%. Found: C, 49.02; H, 6.50; N, 12.51. $C_{27}H_{43}N_6O_5SClCu$ requires C, 49.00; N, 6.55; H, 12.71%; λ_{max}/nm (CH_3CN) 322 (ε/M^{-1} cm^{-1} 12 200), 723 (270), 804 (300). ν_{max}/cm^{-1} (KBr) 3306 (N–H), 2187 (NCO), 1090 (ClO_4), 623 (ν_{ClO_4}); m/z 562 ([M–ClO_4]$^+$, 59%).

[(pbnpa)Cu–N_3]ClO_4 (5)

Yield: 69%. Found: C, 50.48; H, 6.06; N, 15.66. $C_{30}H_{43}N_8O_4SClCu$ requires C, 50.76; H, 6.11; N, 15.80%; λ_{max}/nm (CH_3CN) 325 (ε/M^{-1} cm^{-1} 13 200), 388 (2200), 646 (320), 825 (245); ν_{max}/cm^{-1} (KBr) 3300 (N–H), 2051 (N_3), 1095 (ClO_4), 624 (ClO_4).

[(ebnpa)Cu–N_3]ClO_4 (6)

Yield: 91%. Found: C, 47.43; H, 6.45; N, 16.65. $C_{26}H_{43}N_8O_4SClCu$ requires C, 47.19; H, 6.55; N, 16.94%; λ_{max}/nm (CH_3CN) 325 (ε/M^{-1} cm^{-1} 12 700), 398 (2050), 666 (450), 837 (420); ν_{max}/cm^{-1} (KBr) 3266 (N–H), 2061 (N_3), 1090 (ClO_4), 624 (ClO_4); m/z (relative intensity): 562 ([M–ClO_4]$^+$, 12%).

X-ray crystal structure determinations

Crystal data, data collection, and refinement parameters for **1**, **2**, **3**, and **6** are given in Table 1. The CCDC references are 209457–209460; see http://www.rsc.org/suppdata/dt/b3/b304846b/ for crystallographic data in CIF format.

A crystal of each compound **1**, **2**, **3**, and **6** was mounted on a glass fiber with traces of viscous oil and then transferred to a Nonius KappaCCD diffractometer with Mo Kα radiation (λ = 0.71073 Å) for data collection at 150(1) K (**2**, **3**, and **6**) or 200(1) K (**1**). For each compound, an initial set of cell constants was obtained from ten frames of data that were collected with an oscillation range of 1° frame^{-1} and an exposure time of 20 s frame^{-1}. Indexing and unit cell refinement based on observed reflections from those ten frames indicated monoclinic *P* lattices for **1** and **3**, and triclinic *P* lattices for **2** and **6**. Final cell constants for each complex were determined from a set of strong reflections from the actual data collection. For each data set, reflections were indexed, integrated, and corrected for Lorentz polarization and absorption effects using DENZO-SMN and SCALEPAC.[24] The structures were solved by a combination of direct methods and heavy atom using SIR 97 (Release 1.02).[25] All of the non-hydrogen atoms were refined with anisotropic displacement coefficients. Unless otherwise stated, hydrogen atoms were assigned isotropic displacement coefficients U(H) = 1.2U(C) or 1.5U(Cmethyl), and their coordinates were allowed to ride on their respective carbons using SHELXL-97.[26]

Crystals of **1** were determined to belong to the monoclinic crystal system. Systematic absences in the data were consistent with the space group $P2_1/c$. All hydrogen atoms were located and refined independently. Two oxygen atoms of the perchlorate anion were found to be disordered over two positions (0.81 : 0.19 occupancy ratio), whereas the fourth oxygen was best fit over three positions (0.40: 0.40: 0.20). Complex **2** crystallizes in the space group $P\bar{1}$. All hydrogen atoms were located and refined independently. The cyanate derivative **3** crystallizes in the space group $P2_1/c$. All hydrogen atoms were located and refined independently. The azide complex **6** crystallizes in the space group $P\bar{1}$. Hydrogen atoms were located and refined independently except those on C(14) and C(24), which were assigned isotropic displacement coefficients and their coordinates were allowed to ride on their respective carbons.

Acknowledgements

We acknowledge the support of the donors of the Petroleum Research Fund (ACS-PRF 36394-G3 to LMB), administered by the American Chemical Society, the National Science Foundation (CAREER Award CHE-0094066 to LMB), the Medical College of Wisconsin (BB), and the National Institutes of Health (RR01008 to National Biomedical EPR Center, Department of Biophysics, Medical College of Wisconsin). KJT and ALF thank the Utah State University Vice-President for Research for funding through the Undergraduate Research & Creative Opportunities (URCO) program.

References and notes

1 (*a*) J. P. Klinman, *Chem. Rev.*, 1996, **96**, 2541; (*b*) S. T. Prigge, R. E. Mains, B. A. Eipper and L. M. Amzel, *Cell. Mol. Life Sci.*, 2000, **57**, 1236.
2 DβM: (*a*) N. J. Blackburn, S. S. Hasnain, T. M. Pettingill and R. W. Strange, *J. Biol. Chem.*, 1991, **266**, 23120; (*b*) PAM: N. J. Blackburn, F. C. Rhames, M. Ralle and S. Jaron, *J. Biol. Inorg. Chem.*, 2000, **5**, 341.
3 S. T. Prigge, A. S. Kolhekar, B. A. Eipper, R. E. Mains and L. M. Amzel, *Science*, 1997, **278**, 1300.
4 X-ray crystallography has been used to characterize both the oxidized and reduced forms of PAM (ref. 3 and S. T. Prigge, A. S. Kolhekar, B. A. Eipper, R. E. Mains and L. M. Amzel, *Nat. Struct. Biol.*, 1999, **6**, 976 . In these studies, Cu–ligand bond lengths showed little difference between the two redox levels of the enzyme. These results contrast with those derived from EXAFS studies wherein significant changes in copper coordination environment have been identified (ref. 2*b*).
5 A weakly coordinated solvent molecule may also be bound to Cu_M in the reduced form of PAM (ref. 2*b*).
6 Several structural/functional models for the Cu_B and Cu_M centers in DβM and PAM supported by mixed nitrogen/sulfur chelate ligands have been reported: (*a*) B. K. Santra, P. A. N. Reddy, M. Nethaji and A. R. Chakravarty, *Inorg. Chem.*, 2002, **41**, 1328; (*b*) B. K. Santra, P. A. N. Reddy, M. Nethaji and A. R. Chakravarty, *Dalton Trans.*, 2001, 3553; (*c*) F. Champloy, N. Benali-Cherif, P. Bruno, I. Blain, M. Pierrot, M. Reglier and A. Michalowicz, *Inorg. Chem.*, 1998, **37**, 3910; (*d*) T. Ohta, T. Tachiyama, K. Yoshizawa, T. Yamabe, T. Uchida and T. Kitagawa, *Inorg. Chem.*, 2000, **39**, 4358; (*e*) M. Kodera, T. Kita, I. Miura, N. Nakayama, T. Kawata, K. Kano and S. Hirota, *J. Am. Chem. Soc.*, 2001, **123**, 7715; (*f*) L. Casella, M. Gullotti, M. Bartosek, G. Pallanza and E. Laurenti, *J. Chem. Soc., Chem. Commun.*, 1991, 1235.
7 Structural/functional models for DβM/PAM supported by non-sulfur-containing chelate ligands have also been reported: (*a*) A. Wada, M. Harata, K. Hasegawa, K. Jitsukawa, H. Masuda, M. Mukai, T. Kitagawa and H. Einega, *Angew. Chem., Int. Ed. Engl.*, 1998, **37**, 798; (*b*) S. Itoh, T. Kondo, M. Komatsu, Y. Ohshiro, C. M. Li, N. Kanehisa, Y. Kai and S. Fukuzumi, *J. Am. Chem. Soc.*, 1995, **117**, 4714; (*c*) S. Itoh, H. Nakao, L. M. Berreau, T. Kondo, M. Komatsu and S. Fukuzumi, *J. Am. Chem. Soc.*, 1998, **120**, 2890; (*d*) I. Blain, M. Pierrot, M. Giorgi and M. Reglier, *C. R. Acad. Sci., Ser. IIc: Chim.*, 2001, **4**, 1; (*e*) I. Blain, M. Giorgi, I. De Riggi and M. Reglier, *Eur. J. Inorg. Chem.*, 2001, 205; (*f*) I. Blain, P. Bruno, M. Giorgi, E. Lojou, D. Lexa and M. Reglier, *Eur. J. Inorg. Chem.*, 1998, 1297; (*g*) P. A. N. Reddy, M. Nethaji and A. R. Chakravarty, *Inorg. Chim. Acta*, 2002, **337**, 450; (*h*) P. A. N. Reddy, R. Datta and A. R. Chakravarty, *Inorg. Chem. Commun.*, 2000, **3**, 322.
8 A. W. Addison, T. N. Rao, J. Reedijk, J. van Rijn and G. C. Verschoor, *J. Chem. Soc., Dalton Trans.*, 1984, 1349.
9 D. K. Garner, S. B. Fitch, L. H. McAlexander, L. M. Bezold, A. M. Arif and L. M. Berreau, *J. Am. Chem. Soc.*, 2002, **124**, 9970.
10 Y. Nishida and K. Takahashi, *Inorg. Chem.*, 1988, **27**, 1406.
11 See for example: (*a*) O. P. Anderson and J. C. Marshall, *Inorg. Chem.*, 1978, **17**, 1258; (*b*) M. Julve, M. Verdaguer, G. De Munno, J. A. Real and G. Bruno, *Inorg. Chem.*, 1993, **32**, 795; (*c*) J. Cheng, F.-L. Liao, T.-H. Lu, P. S. Mukherjee, T. K. Maji and N. R. Chaudhuri, *Acta Crystallogr., Sect. E*, 2001, **57**, m263; (*d*) S. Fox, R. T. Stibrany, J. A. Potenza, S. Knapp and H. J. Schugar, *Inorg. Chem.*, 2000, **39**, 4950; (*e*) M. Kabesová, V. Jorík and M. Dunaj-Jurco, *Acta Crystallogr., Sect. C*, 1993, **49**, 1120; (*f*) F. Valach and M. Dunaj-Jurco, *Acta Crystallogr., Sect. B*, 1982, **38**, 2145; (*g*) T. Rojo, A. Garcia, J. L. Mesa, M. I. Arriortua, J. L. Pizarro and A. Fuertes, *Polyhedron*, 1989, **8**, 97; (*h*) T. Otieno, S. J. Rettig, R. C. Thompson and J. Trotter, *Inorg. Chem.*, 1993, **32**, 4384.
12 (*a*) N. J. Blackburn, D. Collison, J. Sutton and F. E. Mabbs, *Biochem. J.*, 1984, **220**, 447; (*b*) N. J. Blackburn, M. Concannon, S. K. Shahiyan, F. E. Mabbs and D. Collison, *Biochemistry*, 1988, **27**, 6001.
13 M. Harata, K. Hasegawa, K. Jitsukawa, H. Masuda and H. Einaga, *Bull. Chem. Soc. Jpn.*, 1998, **71**, 1031.
14 Z. Dori and R. F. Ziolo, *Chem. Rev.*, 1973, **73**, 247.
15 (*a*) A. Allerhand and P. V. R. Schleyer, *J. Am. Chem. Soc.*, 1963, **85**, 1233; (*b*) T. Steiner, *Acta Crystallogr., Sect. B*, 1998, **54**, 456.
16 R. F. Ziolo, M. Allen, D. D. Titus, H. B. Gray and Z. Dori, *Inorg. Chem.*, 1972, **11**, 3044.
17 R. M. Silverstein and F. X. Webster, *Spectrometric Identification of Organic Compounds*, Wiley, New York, 1998.
18 Methods of EPR spectra simulation employed: (*a*) B. Bennett, W. E. Antholine, V. M. D'souza, G. J. Chen, L. Ustinyuk and R. C. Holz, *J. Am. Chem. Soc.*, 2002, **124**, 13025; (*b*) D. M. Wang and G. R. Hanson, *J. Magn. Reson. A*, 1995, **117**, 1.
19 J. Peisach and W. E. Blumberg, *Arch. Biochem. Biophys.*, 1974, **165**, 691.
20 W. L. F. Armarego and D. D. Perrin, *Purification of Laboratory Chemicals*, Butterworth-Heinemann, Boston, MA, 1996.
21 S. Ranganathan, D. Ranganathan and S. K. Singh, *Tetrahedron Lett.*, 1987, **28**, 2893.
22 M. M. Makowska-Grzyska, P. C. Jeppson, R. A. Allred, A. M. Arif and L. M. Berreau, *Inorg. Chem.*, 2002, **41**, 4872.
23 W. C. Wolsey, *J. Chem. Educ.*, 1973, **50**, A335.
24 Z. Otwinowski and W. Minor, *Methods Enzymol.*, 1997, **276**, 307.
25 A. Altomare, M. C. Burla, M. Camalli, G. L. Cascarano, C. Giacovazzo, A. Guagliardi, A. G. G. Moliterni, G. Polidori and R. Spagna, *J. Appl. Crystallogr.*, 1999, **32**, 115.
26 G. M. Sheldrick, SHELXL-97, Program for refinement of crystal structures, University of Göttingen, Germany, 1997.